Landau-level broadening due to electron-impurity interaction in graphene in strong magnetic fields

C. H. Yang,[1,2] F. M. Peeters,[1,*] and W. Xu[3,4]
[1]*Departement Fysica, Universiteit Antwerpen, Groenenborgerlaan 171, B-2020 Antwerpen, Belgium*
[2]*Faculty of Maths and Physics, Nanjing University of Information Science and Technology, Nanjing 210044, China*
[3]*Institute of Solid State Physics, Chinese Academy of Sciences, Hefei 230031, China*
[4]*Department of Physics, Yunnan University, Kunming 610015, China*
(Received 10 March 2010; revised manuscript received 11 June 2010; published 3 August 2010)

The effect of electron-impurity and electron-electron interactions on the energy spectrum of electrons moving in graphene is investigated in the presence of a high magnetic field. We find that the width of the broadened Landau levels exhibits an approximate $1/B$ dependence near half filling for charged impurity scattering. The Landau-level width, the density of states, and the Fermi energy exhibit an oscillatory behavior as a function of magnetic field. Comparison with experiment shows that scattering with charged impurities cannot be the main scattering mechanism that determines the width of the Landau levels.

DOI: 10.1103/PhysRevB.82.075401 PACS number(s): 72.10.−d, 73.20.At, 81.07.−b

I. INTRODUCTION

Graphene, a new material, was stabilized for the first time several years ago by the team of Prof. Geim and co-workers[1] at the University of Manchester. A graphene crystal consists of a carbon honey comb lattice of hexagons which consists of two sublattices leading to pseudospin degrees of freedom. Its electron transport for Fermi energy $|E_F|<0.8$ eV is essentially governed by the massless Dirac equation with a linear energy dispersion relation around the two nodal points in the Brillouin zone. The carrier density (both electron and hole) can be tuned by the gate voltage. Due to its unique electronic band structure and its potential for applications in nanoelectronic devices,[2,3] it is necessary to explore its fundamental physics in the presence of an electric, magnetic, and/or optical field.

In a quasi-two-dimensional electron gas (2DEG), a magnetic field (B) perpendicular to the two-dimensional sheet leads to Landau-level (LL) quantization with energy $E_N=(N+1/2)\hbar\omega_c$, $N=0,1,2,\ldots$, where ω_c is the cyclotron frequency. The free-electron density of states (DOS) consists of δ functions located at the quantized Landau energies. In real systems, due to the presence of disorder and scattering from, e.g., phonons and impurities, the LLs are broadened which will have a smoothening effect on the singular DOS. In graphene, the energy of the LLs is very different compared to those of a conventional 2DEG: (1) the $N=0$ LL has zero energy and is shared equally by electrons and holes, and (2) the LL energy is proportional to $\sqrt{B}$ rather than B. This results into peculiar and unusual quantum features in two-dimensional transport, e.g., half-integer quantum Hall effect[1,4] and anomalous absorption.[5] In order to explain these phenomena, simple estimations based on a finite impurity scattering rate or scattering time were imposed in order to avoid the singularity in the DOS. For example, a LL broadening of $\Gamma=15$ K($\sim$1.3 meV) was assumed in Refs. 5 and 6 for all LLs when calculating the magneto-optical absorption. Also in calculating the magneto-optical properties of graphene Koshino and Ando[7] used $\Gamma\sim3.9$ meV. Orlita *et al.*[8] estimated the peak widths to be 2–10 meV in order to fit the far-infrared optical absorption. The peak width was measured to have a $\sqrt{B}$ dependence in a weak magnetic field (i.e., $B<1$ T) which approached a sublinear function of $\sqrt{B}$ at higher magnetic fields ($1\ \mathrm{T}<B<4$ T). In the work of Jiang *et al.*[9] a Lorentzian broadening was assumed for the LLs to fit the resonances measured in infrared spectroscopy and they found that the half width nonmonotonically increased with increasing magnetic field ($4\ \mathrm{T}<B<25$ T).

Theoretically, the self-consistent Born approximation (SCBA) was used more than 30 years ago by Ando *et al.*[10,11] when calculating the LL broadening of a 2DEG. In their work, the interaction between different LLs was neglected in the limit of a strong magnetic field. The LL broadening due to long-range impurity potentials was able to qualitatively explain the experimental results.[12] The effect of the coupling between different LLs and the effect of several kinds of scattering mechanics, e.g., electron-impurity (e-i) and electron-phonon interactions were investigated in Refs. 13 and 14. In graphene, in the absence of a magnetic field, Hu *et al.*[15,16] used the Born approximation and SCBA to calculate the DOS and the single-particle relaxation time in the presence of disorder due to charged impurity and short-range defect scattering. And in the presence of a magnetic field Peres *et al.*[17] calculated the DOS taking into account vacancy impurity scattering within a single impurity T matrix approximation. In their work, short-range impurity scatterers were assumed and the Fourier transform of the impurity potential V was assumed to be a constant, $V_q\sim V$, i.e., independent of q which is totally different from ionized impurity scattering where $V_q=2\pi e^2/\kappa q$ in the absence of static screening. The LL width as a function of magnetic field was calculated self-consistently. It was found that the ratio $\Gamma/\sqrt{B}$ decreases with increasing B which implies a broadening $\Gamma\sim B^{\alpha}$ with $\alpha<1/2$. The LL width around zero energy was found to be strongly broadened and the LL width away from zero energy was much small. Using the Born approximation[18] and assuming a delta-function scattering potential, the level broadening was found to be proportional to $\sqrt{B}$ and dependent on the impurity density and the effective impurity potential. For intermediate short-range disorder, the $N=0$ LL is well sepa-

rated from the other LLs which is different from the result obtained within the T matrix approximation. The theoretical B dependence and values of the LL width are not good in agreement with the experimental LL width[8,9] in strong magnetic fields. It should be noted that from the linear density dependence of the conductivity of graphene it was concluded that the relevant disorder is due to charged impurities.[19] This conclusion is currently under debate[20] which motivated us to investigate whether the magnetic field dependence of the width of the DOS can contribute to this discussion. Different from previous works we also investigate the effect of LL coupling on our result.

Motivated by the experimental and theoretical works mentioned above, we use the Green's-function approach in this paper in order to give a more detailed analysis of the effect of charged impurity scattering on the high magnetic field DOS. In the present work, first we assume that the impurity-induced disorder is sufficiently weak, such that we may rely on single impurity scattering and average over a random distribution of impurities. We derive the full Green's function instead of the bare Green's function through the self-energy. Second, the magnetic field is taken sufficiently strong that scattering between different LLs can be neglected. Third, the impurities are distributed randomly and homogeneously. The full q dependence of the Fourier transformed e-i interaction in q representation is taken into account and we consider Coulomb impurity scattering. Intraband electron-electron (e-e) screening is considered which implies that the singularity at small q is removed. The broadened LL width is determined self-consistently. In contrast with previous works, we do not assume any particular functional form for the broadened LL and take the full q dependence of the impurity potential into account.

The paper is organized as follows. In Sec. II we define the retarded Green's function of the density-density (d-d) correlation function. The e-e screening and the dynamical dielectric function are obtained within the random-phase approximation (RPA). Then the self-energy induced by impurity scattering are presented. The numerical results are discussed in Sec. III. The conclusions are summarized in Sec. IV where we relate our theoretical results with experiments.

II. THEORETICAL APPROACHES

Here we consider a configuration where the graphene sheet is in the xy plane and the uniform static magnetic field with strength B is applied along the z direction. A carrier in monolayer graphene can be described by Weyl's equation for a massless neutrino.[21,22] Thus, the single-particle Hamiltonian describes a carrier in the π bands near the K point of graphene which can be obtained from, e.g., the $\mathbf{k}\cdot\mathbf{p}$ approach.[21] $\mathbf{k}=(k_x,k_y)\rightarrow\mathbf{k}+e\mathbf{A}/\hbar$ is the wave-vector operator along the 2D plane, and $\mathbf{A}=(0,Bx,0)$ is the vector potential of the applied perpendicular magnetic field in the usual Landau gauge. The corresponding Schrödinger equation $H_0\Psi(x,y)=E\Psi(x,y)$ can be solved analytically. The wave function and energy spectrum for a carrier in graphene are obtained, respectively, as[23]

$$|\alpha\rangle = \Psi_\alpha(\mathbf{r}) = C_N e^{-iyX/l_B^2}\begin{bmatrix} S_N h_{|N|-1}(x-X) \\ h_{|N|}(x-X) \end{bmatrix} \quad (1)$$

and

$$\varepsilon_\alpha = \varepsilon_N = S_N\sqrt{|N|}\hbar\omega_B. \quad (2)$$

Here, $\mathbf{r}=(x,y)$ is the 2D spatial coordinate, the electronic states for a carrier are specified by the set of quantum numbers $\alpha=(N,X)$, where $N(=0,\pm1,\ldots)$ is the LL index, $C_N=\sqrt{(1+\delta_{N,0})/2}$, $X=k_y l_B^2$ relates to the carrier wavevector along the y direction, $l_B=(\hbar/eB)^{1/2}$ is magnetic length, $\hbar\omega_B=\sqrt{2}\gamma/l_B$ is the effective magnetic energy, γ is the band parameter, and $h_N(x)=i^N(2^N N!\sqrt{\pi}l_B)^{-1/2}e^{-x^2/2l_B^2}H_N(x/l_B)$, where $H_N(x)$ is the Hermite polynomial. Furthermore, $S_N=1$ for an electron when $N>0$, $S_N=-1$ for a hole when $N<0$, and $S_N=0$ for $N=0$. The $N=0$ LL is both the bottom of the conduction band and the top of the valence band in graphene which is gapless. In graphene, the Zeeman spin splitting is relatively weak and, therefore, we neglect the Zeeman effect in the present study.

From the wave function and energy spectrum of the carrier, the carrier d-d correlation function (or pair bubble) can be derived. To study the electronic and optical properties of monolayer graphene in a quantizing magnetic field, it is convenient to derive the pair bubble in $(\mathbf{q},t)$ representation. In such a case, the carrier d-d correlation function is defined as

$$\Pi(\mathbf{q},t) = \frac{\Theta(t)}{i\hbar}\frac{g_s g_v}{2\pi l_B^2}\sum_{\alpha',\alpha}\langle[\rho_{\alpha'\alpha}(\mathbf{q},t),\rho_{\alpha\alpha'}(-\mathbf{q},0)]\rangle, \quad (3)$$

where g_s and g_v are the spin and valley degeneracy $g_s=g_v=2$, $D_0=(2\pi l_B^2)^{-1}$ is the degeneracy of each LL, $\rho_{\alpha'\alpha}(\mathbf{q},t)=D_{\alpha'\alpha}(\mathbf{q})e^{i(\varepsilon_{\alpha'}-\varepsilon_\alpha)t/\hbar}c_{\alpha'}^\dagger c_\alpha$ is the space Fourier transform of the density-matrix element, $c_\alpha^\dagger(c_\alpha)$ is the creation (annihilation) operator for a carrier in LL state α, and $D_{\alpha'\alpha}(\mathbf{q})=\langle\alpha'|e^{-i\mathbf{q}\cdot\mathbf{r}}|\alpha\rangle$. Due to the relation $\langle[c_{\alpha'}^\dagger c_\alpha, c_\alpha^\dagger c_{\alpha'}]\rangle=f(\varepsilon_{\alpha'})-f(\varepsilon_\alpha)$ with $f(x)$ being the Fermi-Dirac function, the time Fourier transform of the d-d correlation function is rewritten as

$$\Pi(q,\Omega) = \frac{g_s g_v}{2\pi l_B^2}\sum_{N',N} C_{N'N}(u)\frac{f(\varepsilon_{N'})-f(\varepsilon_N)}{\hbar\Omega+\varepsilon_{N'}-\varepsilon_N+i\delta}, \quad (4)$$

where $u=l_B^2q^2/2$ and $C_{N'N}(u)=C_{N'}^2C_N^2[M!/(M+J)!]e^{-u}u^J\times[L_M^J(u)+S_{N'}S_N\sqrt{\frac{M+J}{M}}L_{M-1}^J(u)]^2$, with $M=\min(|N'|,|N|)$, $J=||N'|-|N||$, and $L_N^J(x)$ being the associated Laguerre polynomial. $\hbar\Omega$ is the electronic excitation energy, and an infinitesimal quantity $i\delta$ is introduced to make the integral converge when doing the Fourier transform from time representation to energy representation.

In the present work, we assume that the Fermi energy is in the conduction band, i.e., the carriers are electrons. For the case the e-e interaction is given by the Coulomb potential, the space Fourier transform of the scattering energy for bare e-e interaction is $V_q=2\pi e^2/(\kappa q)$ with κ the static dielectric constant for electrons in graphene. Under the usual RPA, the

effective e-e interaction can be obtained as $V_q^{eff}=V_q/\epsilon(q)$, where $\epsilon(q)=\epsilon(q,\Omega=0)=1-V_q\Pi(q,\Omega)$ is the static dielectric function.[24,25]

Here we consider the case that the LL broadening is mainly induced by scattering with charged impurities, e.g., coming from localized charges in the substrate that supports the graphene monolayer and/or charged adsorbates. When the e-i scattering is given by the Coulomb potential, the interaction Hamiltonian is

$$H_{e-i}=\frac{Ze^2}{\kappa_1}\frac{1}{|\mathbf{R}-\mathbf{R}_a|}, \tag{5}$$

where $\mathbf{R}=(\mathbf{r},0)$ is the coordinate of a carrier in the graphene layer and the impurity with charge number Z is located at $\mathbf{R}_a=(\mathbf{r}_a,z_a)$. κ_1 is the dielectric constant for impurities in the SiO_2 wafer. After assuming that the system can be separated into carriers of interest $|\alpha\rangle$ and impurities $|I\rangle$ which are distributed randomly in the xy plane, namely, $|\alpha;I\rangle=|\alpha\rangle\otimes|I\rangle$, the matrix element for e-i interaction is obtained, in the absence of e-e screening, as

$$V_{\alpha'\alpha}(q,\mathbf{R}_a)=V_q^i D_{\alpha'\alpha}(\mathbf{q})e^{-q|z_a|}e^{i\mathbf{q}\cdot\mathbf{r}_a}\langle I'|I\rangle, \tag{6}$$

where $\langle I'|I\rangle=\sqrt{n_i(z_a)}$ with $n_i(z_a)$ being the charged impurity distribution along the z direction, $\mathbf{q}=(q_x,q_y)$ is the change in the carrier wave vector during an e-i scattering event, and $V_q^i=2\pi Ze^2/\kappa_1 q$. Here, we consider the charged impurities spatially separated from the graphene layer and situated in a 2D layer at a distance d from graphene, the square of the matrix element for e-i scattering in the presence of e-e screening[14,24,26] is obtained as

$$|U_{N'N}(q)|^2=n_i\left(\frac{2\pi Ze^2}{\kappa_1(q+K_q)}e^{-qd}\right)^2 C_{N'N}(l_B^2q^2/2), \tag{7}$$

where $n_i=\int dz_a n_i(z_a)\delta(z_a-d)$. $K_q=(-2\pi e^2/\kappa)\mathrm{Re}\,\Pi(q)$ is the RPA inverse screening length with $\Pi(q)=\lim_{\Omega\to 0}\Pi(\mathbf{q},\Omega)$. It should be noted that e-e scattering at the Fermi level is basically elastic. As a result, the RPA screening length is mainly determined by the intra-LL (i.e., $N'=N$) scattering channels at low temperature $T\to 0$ and in the limit of long-range scattering.[26–28] In such a case, $-\partial f/\partial\varepsilon_N\to\delta(E_F-\varepsilon_N)\to-(1/\pi)\mathrm{Im}\,G_N(E_F)$ and the RPA inverse screening length becomes

$$K_q\simeq-\frac{g_s g_v e^2}{\pi\kappa l_B^2}\sum_N C_{NN}(l_B^2q^2/2)\mathrm{Im}\,G_N(E_F). \tag{8}$$

With the e-i interaction matrix, the self-energy induced by e-i scattering can be evaluated within the Born approximation,[13,14] which reads

$$\Sigma_N(E)=\sum_{N',\mathbf{q}}|U_{N'N}(q)|^2 G_{N'}(E), \tag{9}$$

where E is the carrier energy and

$$G_N(E)=[E-\varepsilon_N-\Sigma_N(E)]^{-1} \tag{10}$$

is the Green's function. The self-energy for a carrier in the Nth LL can be written as

$$\Sigma_N(E)=\Delta_N(E)-i\Gamma_N(E), \tag{11}$$

where the real part $\Delta_N(E)$ results in an energy shift and the imaginary part $\Gamma_N(E)$ determines the width of the LL. From Eqs. (10) and (11), the real and imaginary parts of the Green's function for a carrier in the Nth LL can be obtained straightforwardly.

Because e-i interaction basically is an elastic-scattering mechanism, the self-energy induced by e-i scattering is mainly determined by intra-LL transition processes at least in a strong magnetic field where the LLs do not overlap.[12,18,26,27] In such a case, neglecting the interaction between different LLs, we only consider $N=N'$ in Eq. (9) which results in

$$\Delta_N(E)=(E-\varepsilon_N)/2,$$

$$\Gamma_N(E)=\mathrm{Re}\sqrt{(\Gamma_N)^2-(E-\varepsilon_N)^2/4},$$

and

$$\mathrm{Im}\,G_N(E)=-\frac{1}{\Gamma_N}\mathrm{Re}\left[1-\left(\frac{E-\varepsilon_N}{2\Gamma_N}\right)^2\right]^{1/2} \tag{12}$$

which is a semielliptic type of LL broadening, where

$$\Gamma_N^2=\sum_{\mathbf{q}}|U_{NN}(q)|^2 \tag{13}$$

is given by Eq. (7). It can be seen that the level broadening depends strongly on the scattering potential and the impurity distribution. The DOS for carriers in the Nth LL is then given by

$$D_N(E)=\frac{g_s g_v}{2\pi l_B^2}(-1/\pi)\mathrm{Im}\,G_N(E). \tag{14}$$

From the above analysis, the LL broadening is determined by the screened e-i scattering. And the inverse screening length is determined by the imaginary part of the Green's function (or DOS) which in its turn is determined by the broadened LL width. So the spectrum of broadened LLs and the DOS should be calculated self-consistently. First, at a fixed magnetic field B and electron density n_e, we assume an initial value for the LL width, and the imaginary part of the Green's function [Eq. (12)] and the DOS [Eq. (14)] can be derived straightforwardly. Second, the Fermi energy of this system can be determined from the condition of electron number conservation $n_e=\Sigma_N\int_E dE f(E)D(E)$. Third, the RPA inverse screening length K_q is obtained from Eq. (8). Fourth, the potential induced by the screened impurity scattering gives a new value for the widths of the LLs from Eq. (13). Then, the new imaginary part of the Green's function, E_F and K_q and new broadening width can be obtained until E_F and $\Sigma_N(E)$ are converged. In this way, the width of the LLs in the presence of the screened e-i scattering is obtained iteratively.

III. RESULT AND DISCUSSION

For the numerical calculation, we take the band parameter $\gamma=6.5$ eV Å for graphene, the static dielectric constant for electrons in graphene $\kappa=2.5$ and for impurities in the SiO_2

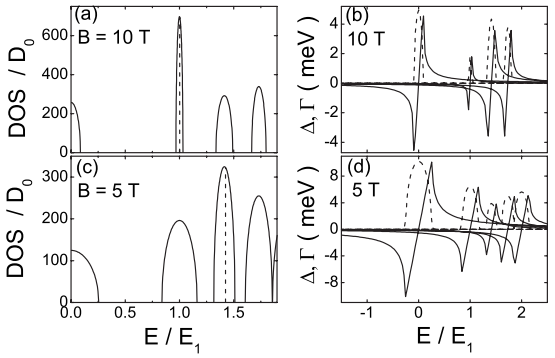

FIG. 1. [(a) and (c)] The DOS and [(b) and (d)] the Landau-level width $\Gamma_N(E)$ (dashed curves) and the energy shift $\Delta_N(E)$ (solid curves) as a function of energy for a fixed electron density $n_e = 10^{12}$ cm^{-2} and impurity density $n_i = 10^{11}$ cm^{-2}. $D_0 = (2\pi l_B^2)^{-1}$ is the degeneracy of each LL. The vertical dashed lines in (a) and (c) indicate the position of the Fermi energy E_F.

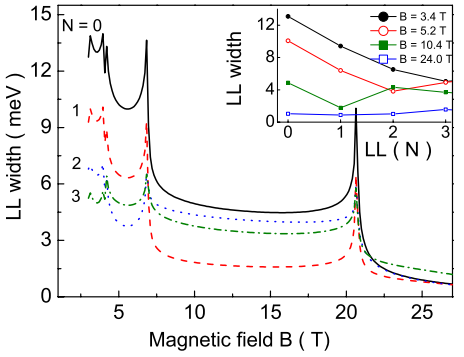

FIG. 2. (Color online) The width of the Nth LL as a function of magnetic field at a fixed electron density $n_e = 10^{12}$ cm^{-2} and impurity density $n_i = 10^{11}$ cm^{-2}. Solid line (black), dashed line (red), dotted line (blue), and dashed-dotted line (olive) are for the $N=0$, 1, 2, and 3 LLs, respectively. The inset shows the width of different LLs for different values of B.

substrate $\kappa_1 = 4.25$. We consider an electron density $n_e \sim 10^{12}$ cm^{-2} whose value can be tuned by the gate voltage. The charged impurities are assumed to be located in the substrate separated from the 2D graphene interface by $d \sim 1$ nm with the impurity density $n_i \sim 10^{11}$ cm^{-2}. In the calculation, we take $Z=1$ for the charge impurity.

In Fig. 1 we show the DOS for two values of the magnetic field. Let us first focus our attention to the LL broadening at a fixed magnetic field. In Fig. 1 the restriction $\Gamma \ll \hbar\omega_B$ is satisfied in the presence of a strong magnetic field. However, because the LL energy is proportional to $\sqrt{|N|}$, the spacing between subsequent LLs $(\sqrt{|N+1|} - \sqrt{|N|})\hbar\omega_B$ decreases with N, which behaves as $\hbar\omega_B/2\sqrt{N}$ for large N. Thus if the LL width would be independent of N these levels will start to overlap beyond a certain LL.

Similar for the case of a normal 2DEG we find that the DOS oscillates as a function of energy and the peaks of the DOS are centered around ε_N but the overall magnetic field dependence is very different. The e-i potential V_q depends on the modulus $q = \sqrt{q_x^2 + q_y^2}$. When an electron is scattered by a single impurity, momentum conservation is required $\delta_{k_y = k'_y - q_y}$, where k_y and k'_y are the electrons momentum before and after scattering, and q_y is the change in the carrier wave vector. The summation over the states (N, k'_y) in the self-energy is related with q_y, which is connected to the scattering potential V_q. This q dependence of the self-energy causes a different broadening for the various LLs. And neglecting the interaction between different LLs, the oscillation of the associated Laguerre polynomial results in a small broadening of the LL at the Fermi energy (E_F). The corresponding broadening width $\Gamma_N(E)$ and the energy shift $\Delta_N(E)$ for different LLs are plotted as a function of energy in Figs. 1(b) and 1(d). At the center of each LL, a peak in $\Gamma_N(E)$ occurs and $\Delta_N(E)$ changes sharply. This is different from Ref. 17, where short-range e-i scattering was assumed and the self-energy $\Sigma_1(E)$ for the $N=0$ LL was calculated and $\Sigma_2(E)$ was taken for the other LLs. The imaginary part of their self-energy showed a single broadened peak at zero energy which smeared the $N=0, \pm 1$ LLs. Their self-energy was independent of the LL number (except for the $N=0$ LL) and as a consequence they found that the energy shift and the broadening of each LL did not exhibit any obvious oscillatory behavior as a function of the LL energy.

In Fig. 2, we show the self-consistent widths of the broadened LLs at a fixed electron density $n_e = 10^{12}$ cm^{-2}. We notice the following: first, periodic oscillations are observed. When the Fermi energy determined by the electron number conservation is in the middle of a broadened LL, screening is the most effective which results in a smaller width. When N LLs are fully occupied and the $(N+1)$th LL is empty, the absolute value for the imaginary part of the Green's function at the Fermi energy is small in Eq. (12) with a small RPA inverse screening length in Eq. (8). In this situation, screening is weak and the e-i interaction gives rise to a large width. Second, the degeneracy $D_0 = (2\pi l_B^2)^{-1}$ of each LL is proportional to the magnetic field and the inverse screening length, on the average, increases with B. This implies that the effect of screening is stronger with increasing B. Third, ignoring the LL overlap in the self-energy calculation, the oscillation of the associated Laguerre polynomial in the coefficient $C_{N,N'}(l_B^2 q^2/2)$ as a function of $l_B q$ leads to a minimal value for the width at E_F. This feature can be clearly seen in the inset in Fig. 2. The inset shows the different LL widths for four values of the magnetic field taken at near half-filling occupation. The highest occupied LL is $N=3$, 2, 1, and 0 at $B=3.4$ T, 5.2 T, 10.4 T, and 24.0 T, respectively. The width of the LL is minimum at the Fermi energy.

Figure 3 shows clearly the close relation between the filling factor and the periodic variation in the DOS and the LL width at the Fermi energy with the magnetic field. The DOS (E_F), the LL width at E_F, and the self-consistent Fermi energy near integer LL filling exhibit strong variations with magnetic field. In Ref. 26, the LL width was calculated in case of Coulomb e-i interaction and e-e screening was considered to remove the divergence in the LL width's calculation. They simplified the polarization function, proportional to Γ^{-1}, and obtained the broadening Γ which increased monotonically with $l_B \sim 1/\sqrt{B}$. In the present paper, the inverse screening length is a function of Γ in Eqs. (8) and (12) and is proportional to Γ^{-1} at $E = \varepsilon_N$, i.e., at half filling. Apart

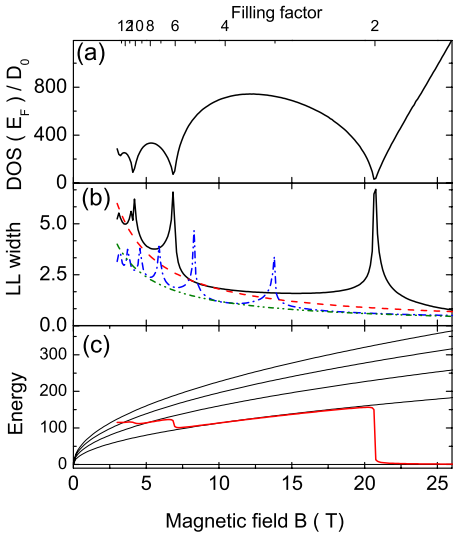

FIG. 3. (Color online) (a) The DOS at the Fermi energy $D(E_F)$, (b) the LL width at E_F, and (c) the LL energy in units of millielectron volt as a function of magnetic field (or filling factor) for $n_e=10^{12}$ cm^{-2} and $n_i=10^{11}$ cm^{-2}. The dashed line (red) in (b) fits the width dependence $\sim B^{-1}$ near half filling. The solid thick line (red) in (c) is the Fermi energy. The curves (blue dashed-dotted and olive dashed-dotted-dotted curves) in (b) are the result for $n_e=2\times10^{12}$ cm^{-2} and $n_i=0.5\times10^{11}$ cm^{-2}.

from the peak structure in the LL width at E_F our result indicates that this width (i.e., near half filling) decreases with increasing magnetic field and can be fitted approximately to $\sim B^{-1}$ [see the red dashed and the olive dashed-dotted-dotted curves in Fig. 3(b)]. Away from half filling, the screening effect decreases which results in an increase in Γ and an oscillatory behavior as a function of B. Near integer filling, the screening length is very weak and is not able to remove the divergence which implies that other short-range scattering should be included. Our results are markedly different from those of delta-function scattering where it was found $\Gamma\sim\sqrt{B}$ in the Born approximation and $\Gamma\sim B^{\alpha}$ with $\alpha<1/2$ in the T matrix approximation. In Fig. 3(b) we plotted the LL width at E_F for $n_e=2\times10^{12}$ cm^{-2} and $n_i=0.5\times10^{11}$ cm^{-2}. In order that the LL does not overlap at high energy, the LL width should be smaller than $\hbar\omega_B/2\sqrt{N}\sim\sqrt{B/N}$ for large N. Therefore, for the higher electron-density case, we reduced the impurity density by a factor of 2. The $\Gamma\sim B^{-1}$ dependence is found in both cases.

The value of the LL width is a function of n_e, n_i, B and E_F. And Γ is proportional to $\sqrt{n_i}$ [see Eq. (7)], and thus increasing the impurity density will obviously increase the LL width. In Fig. 4 the DOS of each LL is shown for the case of a higher impurity density at a fixed magnetic field. The self-consistent DOS is much broader and the LL overlap is significant in this case, in particular, at relative low magnetic field. The total DOS shows substructure between the LLs in Fig. 4(c). The corresponding self-energy is plotted in Figs. 4(b) and 4(d). Increasing the charged impurity density, the real and imaginary parts of the self-energy increases which causes the LLs to overlap and coupling between the LLs should be included. The effect of such coupling is investigated in Fig. 5 where we compare the DOS in the absence

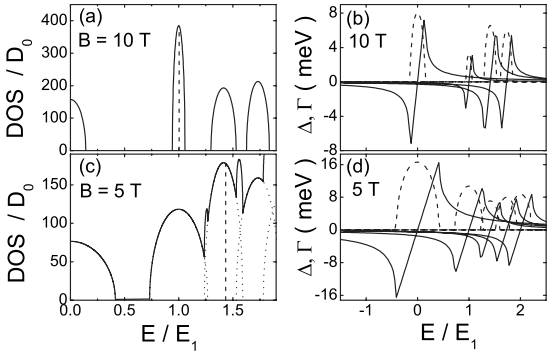

FIG. 4. [(a) and (c)] The DOS and [(b) and (d)] the Landau-level width $\Gamma_N(E)$ (dashed lines) and the energy shift $\Delta_N(E)$ (solid lines) as a function of energy for the same parameters as in Fig. 1 except for a higher impurity density $n_i=2\times10^{11}$ cm^{-2}. The bold solid line in (c) is the total DOS. The vertical dashed lines in (a) and (c) indicate the position of the Fermi energy E_F.

[Fig. 4(c)] and the presence (Fig. 5) of LL coupling. When the inter-LL coupling with ten adjacent LLs [i.e., including $U_{N,N}, U_{N,N\pm1}, \ldots, U_{N,N\pm10}$ in the self-energy of Eq. (9)] are included, the DOS is determined by $\Gamma_{N,N}$ and the adjacent $\Gamma_{N,N'}$ for energies near the center of each LL. From Fig. 5 we can clearly see that this LL coupling has a very small effect on the $N=0$ and $N=1$ LLs which are still well separated from the other LLs. The DOS for the other LLs are more strongly influenced by the coupling between different LLs but the overall effect is not large. Notice also that applying a strong magnetic field, the degeneracy increases which increases the screening effect and subsequently decreases the LL width. This is the reason why at high magnetic fields the overlap between LLs can decrease.

IV. CONCLUSION

At low temperatures, e-i scattering is believed to be the principal channel for electron momentum relaxation in graphene that is supported by SiO_2. In this paper, a detailed self-consistent calculation method was applied to calculate the Green's function, self-energy, and the DOS in the pres-

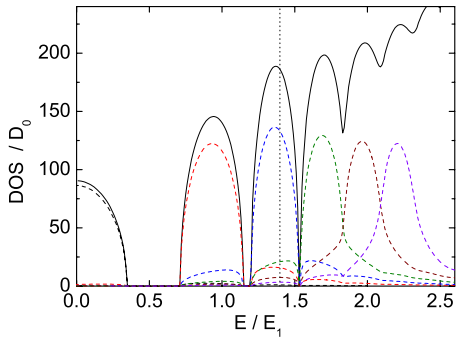

FIG. 5. (Color online) The DOS as a function of energy for the same parameters as in Fig. 4(c) including the coupling between ten adjacent LLs. The solid (black) curve indicates the total DOS and the dashed (color) curves are the DOS of each LL. The vertical dotted line indicates the position of the Fermi energy.

ence of a strong magnetic field and charged impurity scattering. In our numerical self-consistent calculation we have taken into account intraband screening and neglected the interaction between different LLs when the restriction $\Gamma < \hbar\omega_B$ is satisfied. The LL widths are determined which depend on the electron density, magnetic field, impurity density, and the screened e-i coupling strength. When the conditions of strong magnetic field and weak disorder are satisfied, the width of each LL oscillates as a function of magnetic field and/or electron density. Peaks in the LL width Γ are found for electron energy situated between the LLs which are expected to be reduced when including inter-LL e-e screening[29] and short-range e-i scattering.

An approximate dependence $\Gamma \sim 1/B$ is obtained near half filling. A decreasing width with increasing magnetic field is in disagreement with experimental results from magneto-optical properties.[8,9] The experimental LL width in high magnetic fields shows a sublinear $\sqrt{B}$ dependence[8] and nonmonotonically increasing with magnetic field.[9] Thus we have to conclude that charged impurity scattering cannot be the main mechanism that determines the broadening at high magnetic fields. Therefore, it is expected that other scattering mechanisms will be very important in the determination of the width of the LLs. The screened e-i potential depends on q and as a consequence it contributes differently to each LL width, which differs from the case of the short-range scattering model presented by Peres *et al.*[17] The LL width at E_F exhibits smaller broadening as compared to the neighbor LLs. Because e-i scattering strength is proportional to the square root of the impurity density, i.e., $\sqrt{n_i}$, broader LLs are observed in the case of high-impurity concentrations which eventually may lead to coupling between different LLs. We found that the scattering between different LLs in this case has only a small effect on the DOS especially for low LLs. Note that the Landau widths is not exactly linearly proportional to $\sqrt{n_i}$ because the widths, the DOS, and the Fermi energy are determined by several parameters, i.e., n_e, B, and n_i in a self-consistent way.

ACKNOWLEDGMENTS

This work was supported by the Flemish Science Foundation (FWO-Vl), the Belgian Science Policy (IAP), the National Science Foundation of China under Grant No. 10804053, the Foundation of NUIST under Grant No. S8108062001, and the Chinese Academy of Sciences and Department of Science and Technology of Yunnan Province.

*francois.peeters@ua.ac.be

[1] K. S. Novoselov, A. K. Geim, S. V. Morozov, D. Jiang, M. I. Katsnelson, I. V. Grigorieva, S. V. Dubonos, and A. A. Firsov, Nature (London) **438**, 197 (2005).
[2] K. S. Novoselov, A. K. Geim, S. V. Morozov, D. Jiang, Y. Zhang, S. V. Dubonos, I. V. Grigorieva, and A. A. Firsov, Science **306**, 666 (2004); Y. Zhang, J. P. Small, M. E. S. Amori, and P. Kim, Phys. Rev. Lett. **94**, 176803 (2005).
[3] Y. Zhang, J. P. Small, W. V. Pontius, and P. Kim, Appl. Phys. Lett. **86**, 073104 (2005).
[4] Y. Zhang, Y.-W. Tan, H. L. Stormer, and P. Kim, Nature (London) **438**, 201 (2005).
[5] V. P. Gusynin, S. G. Sharapov, and J. P. Carbotte, Phys. Rev. Lett. **98**, 157402 (2007).
[6] V. P. Gusynin, S. G. Sharapov, and J. P. Carbotte, J. Phys.: Condens. Matter **19**, 026222 (2007).
[7] M. Koshino and T. Ando, Phys. Rev. B **77**, 115313 (2008).
[8] M. Orlita, C. Faugeras, P. Plochocka, P. Neugebauer, G. Martinez, D. K. Maude, A.-L. Barra, M. Sprinkle, C. Berger, W. A. de Heer, and M. Potemski, Phys. Rev. Lett. **101**, 267601 (2008).
[9] Z. Jiang, E. A. Henriksen, L. C. Tung, Y. J. Wang, M. E. Schwartz, M. Y. Han, P. Kim, and H. L. Stormer, Phys. Rev. Lett. **98**, 197403 (2007).
[10] T. Ando and Y. Uemura, J. Phys. Soc. Jpn. **36**, 959 (1974).
[11] T. Ando, A. B. Fowler, and F. Stern, Rev. Mod. Phys. **54**, 437 (1982).
[12] W. Cai and C. S. Ting, Phys. Rev. B **33**, 3967 (1986).
[13] X. C. Xie, Q. P. Li, and S. Das Sarma, Phys. Rev. B **42**, 7132 (1990).
[14] W. Xu and P. Vasilopoulos, Phys. Rev. B **51**, 1694 (1995).
[15] Ben Yu-Kuang Hu, E. H. Hwang, and S. Das Sarma, Phys. Rev. B **78**, 165411 (2008).
[16] E. H. Hwang and S. Das Sarma, Phys. Rev. B **77**, 195412 (2008).
[17] N. M. R. Peres, F. Guinea, and A. H. Castro Neto, Phys. Rev. B **73**, 125411 (2006).
[18] N. H. Shon and T. Ando, J. Phys. Soc. Jpn. **67**, 2421 (1998).
[19] B. Huard, N. Stander, J. A. Sulpizio, and D. Goldhaber-Gordon, Phys. Rev. B **78**, 121402(R) (2008).
[20] L. A. Ponomarenko, R. Yang, T. M. Mohiuddin, M. I. Katsnelson, K. S. Novoselov, S. V. Morozov, A. A. Zhukov, F. Schedin, E. W. Hill, and A. K. Geim, Phys. Rev. Lett. **102**, 206603 (2009).
[21] J. W. McClure, Phys. Rev. **104**, 666 (1956).
[22] T. Ando, J. Phys. Soc. Jpn. **74**, 777 (2005).
[23] See, e.g., T. Ando, J. Phys. Soc. Jpn. **76**, 024712 (2007).
[24] E. H. Hwang and S. Das Sarma, Phys. Rev. B **75**, 205418 (2007).
[25] R. Roldán, M. O. Goerbig, and J.-N. Fuchs, Semicond. Sci. Technol. **25**, 034005 (2010).
[26] K. Nomura and A. H. MacDonald, Phys. Rev. Lett. **96**, 256602 (2006).
[27] Y. Murayama and T. Ando, Phys. Rev. B **35**, 2252 (1987).
[28] A. V. Khaetskii and Y. V. Nazarov, Phys. Rev. B **59**, 7551 (1999).
[29] I. V. Gornyi, A. D. Mirlin, and F. von Oppen, Phys. Rev. B **70**, 245302 (2004).